Journal of Magnetics 16(2), 108-113 (2011) DOI: 10.4283/JMAG.2011.16.2.108

Magnetic Properties of Cr-doped $LiNbO_3$ by Using the Projection Operator Technique

Jung-Il Park[1], Hyeong-Rag Lee[1]*, and Haeng-Ki Lee[2]

[1]Nano Practical Application Physics Lab, Department of Physics, Kyungpook National University, Daegu 702-701, Korea
[2]Department of Radiotechnology, Daegu Polytechnic College University, Daegu 706-711, Korea

(Received 11 March 2011, Received in final form 1 May 2011, Accepted 3 May 2011)

The electron spin resonance lineshape (ESRLS) function for the electron spin resonance linewidth (ESRLW) of Cr^{3+} (S = 3/2) in ferroelectric lithium niobate single crystals doped with 0.05 wt% of Cr, is obtained by using the projection operator technique (POT), developed by Argyres and Sigel. The ESRLS function is calculated to be axially symmetric about the c – axis and analyzed by using the spin Hamiltonian $H_{SP} = \mu_B (\vec{B} \cdot \vec{\vec{g}} \cdot \vec{S}) + \vec{S} \cdot \vec{\vec{D}} \cdot \vec{S}$ with the parameters g = 1.972 and D = 0.395 cm^{-1}. In the *ca* plane, the linewidths show a strong angular dependence, whereas in the *ab* plane, they are independent of the angle. This result implies that the resonance center has an axial symmetry along the c – axis. Further, from the temperature dependence of the linewidths that is shown, it can be seen that the linewidths increase as the temperature increases, at a frequency of ν = 9.27 GHz. This result implies that the scattering effect increases with increasing temperature. Thus, the POT is considered to be more convenient to explain the scattering mechanism as in the case of other optical resonant systems.

Keywords : electron spin resonance linewidth (ESRLW), electron spin resonance lineshape (ESRLS), spin Hamiltonian, projection operator technique (POT), lithium niobate (LN), dynamical electron spin susceptibility (DESS)

1. Introduction

The generation of electron spin resonance linewidth (ESRLW) in ferroelectric single crystals as a response to a circularly polarized radiation is a topic under extensive experimental and theoretical study [1-3]. The study of magneto-optical transitions of electron spin in crystals has almost always been restricted to the frequency range between far infrared and visible light involving inter-band transitions in ESR. Usually, ESR spectrometers are operated at several fixed frequencies such as the X-band (≈9 GHz) and occasionally at the K- and Q-bands. Trivalent ions, including those of transition metals and rare earth elements, belong to the most important impurities in lithium niobate (LN, $LiNbO_3$). These ions are important because of their critical influence on the properties of LN, such as its domain structure, electro-optical coefficients, light absorption, and refractive indices and their consequences for present and potential applications. The elucidation of the position of impurities in the LN crystals, their nearest surroundings, and the process of change compensation is vital in order to tailor the fundamental properties of LN for various applications. LN crystals have been utilized in ultrasonic transducers [4, 5], electro-optical modulators [6-8], surface acoustic wave devices, etc. They are readily doped with rare earth and transition metal impurities, and the doped crystals have found applications in holographic storage and as laser hosts. ESR is the most direct method for determining the paramagnetic impurity center structure and its characteristics. Taking into account that Cr^{3+} [1-3] is a paramagnetic ion, it is very useful to carry out ESR measurements.

The theoretical studies performed on resonant system in the presence of an external electromagnetic radiation thus far have usually been based on the following methodologies: the Boltzmann transport theory, Green's function approach [9], the force-balance approach, Feynmann's path integral approach, the Stark-ladder representation approach, the Wigner-representation approach, and the projection operator technique (POT) [10-21]. Among these, in this study, we focus on the POT approach of Argyres and Sigel [16]. The projection operator in the method of Argyres and Sigel contains the index of electron spin. While utilizing this method, we succeeded in formulating a response theory [14, 15, 21], which includes the Kubo theory as the lowest-order approximation. The derived lineshape function is similar to those obtained by other methods

*Corresponding author: Tel: +82-53-950-5321
Fax: +82-53-952-1739, e-mail: phyhrlee@knu.ac.kr

[10-13]. Further, it is shown that the amount of calculation involved in the technique of Argyres and Sigel is considerably lesser than that required for other technique. For LN crystal in the presence of a perpendicular static magnetic field, the electron spin resonance lineshape (ESRLS) spectrum, up to a constant factor, can be expressed as

$$\frac{-\mathrm{Im}\Pi_{+-}^{ESR}(\omega)}{[\omega-\omega_z-\mathrm{Re}\Pi_{+-}^{ESR}(\omega)]^2+[\mathrm{Im}\Pi_{+-}^{ESR}(\omega)]^2} \quad (1)$$

where $\mathrm{Re}\Pi_{+-}^{ESR}(\omega)$ and $\mathrm{Im}\Pi_{+-}^{ESR}(\omega)$ are the real and the imaginary parts respectively, of the ESRLS function. The correction to the resonance field can then be determined accurately from the equation $\omega-\omega_z-\mathrm{Re}\Pi_{+-}^{ESR}(\omega)=0$ because $\mathrm{Im}\Pi_{+-}^{ESR}(\omega)$ is a slowly varying function of the angular frequency or the magnetic field.

In this study, for the ESR of Cr^{3+} (S = 3/2) in ferroelectric LN crystals doped with Cr, the ESRLS is obtained using the POT developed by Argyres and Sigel. The ESRLS is calculated to be axially symmetric about the c – axis and analyzed using the spin Hamiltonian with the parameters g = 1.972 and D = 0.395 cm^{-1}. The scattering strength of the ESRLS is expanded in the conventional series representation. On the basis of numerical calculation, we analyzed the temperature and the angular dependence of the ESRLS at a frequency of ν = 9.27 GHz in external electromagnetic radiation.

2. Structure and Lineshape Function

LN's structure at temperatures below its ferroelectric Curie temperature (approximately 1210 ºC) [8] consist of planar sheet of oxygen atoms in a distorted hexagonal close-packed configuration. The octahedral interstices formed in this structure are one-third filled by lithium atoms, one-third filled by niobium atoms, and one-third vacant. In the c direction, the atoms occur in the interstices in the following order:…, Nb, vacancy, Li, Nb, vacancy, Li,…. In the paraelectric phase above the Curie temperature, the Li atoms lie in an oxygen layer that is c/4 away from the Nb atoms are centered between oxygen layer. These positions make the paraelectric phase non-polar. As the temperature decreases from the Curie temperature, the elastic forces of the crystal become dominant and force the lithium and niobium ions into new positions. The charge separation resulting from this shift of ions relative to the oxygen octahedral causes LN to exhibit spontaneous polarization at temperatures below 1210 ºC. LNO crystals are built up of regular arrangements of atoms in three dimensions, these arrangements can be represented by a repeat unit of constituent atoms or ions, which can be understood in terms of packing, linking, or both. As mentioned above, in the LNO crystallographic frame, there are three kinds of constituent octahedra, LiO_6, NbO_6, and $\square O_6$ where $\square$ represents a vacant site. For the ferroelectric phase of LNO crystals, octahedra sharing faces along the c-axis from a helix, while octahedra at the ab plane share their common edges. The basic structure unit of LNO crystals may be regarded as the perfect octahedral without any distortion, the distortion is formed by their different linkages when they stack each other in the real crystallographic frame. Thus, LN belongs to the broad class of displacement ferroelectrics. In the ferroelectric phase a LN crystal exhibits three-fold rotation symmetry about its c – axis. Thus, it is a member of the trigonal crystal system. In addition, it exhibits mirror symmetry about three plans that are 60º apart and intersect forming a three-fold rotation axis. These two symmetry operations then classify LN as a member of the 3m point group. It also belongs to the R3c space group. In the trigonal system, two quite different unit cells can be chosen, hexagonal or rhombohedral. We choose crystal structure in the ferroelectric phase viewed as a hexagonal unit cell for LN. In this unit cell, the c – axis is defined as the axis about which the crystal exhibits three-fold rotation symmetry.

ESRLS is characterized by the imaginary part of the dynamical electron spin susceptibility (DESS) [11]:

$$\chi_{+-}(\omega)=\chi'_{+-}(\omega)+i\chi''_{+-}(\omega) \quad (2)$$

$$\chi''_{+-}(\omega)=\frac{g_e^2\mu_B^2}{4Vh}\lim_{a\to+0}\int_0^\infty dt \exp(-i\omega t-at)\langle[\sigma_-(0),\sigma_+(t)]\rangle_{EA} \quad (3)$$

where $\sigma_\pm(t)=\exp(iLt)\sigma_\pm$, L being the Liouville operator corresponding to the Hamiltonian of the system. Here, V, g_e, μ_B, ω, $\langle\cdots\cdots\rangle_{EA}$ and [,] are the volume of the system, Lande g-factor of an electron in vacuum, Bohr magneton, the frequency of the incident electromagnetic radiation, ensemble average of the system and the usual commutator, respectively. We denote the sum of the spin matrix of the total electrons in the system as $\sigma_\pm=\sigma_x\pm i\sigma_y$. For an external circularly polarized radiation $\vec{H}(t)=H_0[\exp(-i\omega t)+c.c]\hat{z}$ with angular frequency ω applied along the z – axis, we consider the interaction between electron, and describe the system in terms of a Hamiltonian. It consists of three parts: orbital energy, Zeeman energy, and spin denoted as $H=H_F+H_Z+H_s$. Additionally, orbital energy $H_F(10^5\ cm^{-1})$ further consists of four parts, i.e., $H_F=H_K+H_e+H_{ee}+H_{so}$, where H_K, H_e, H_{ee} and $H_{so}(10^2\ cm^{-1})$ are kinetic energy, Coulomb energy, electron-electron interaction and spin-orbit coupling, respectively [22-26],

$$H_F=-\sum_i \frac{\hbar^2}{2m_i}\nabla^2-\frac{1}{4\pi\varepsilon_0}\sum_i\frac{Ze^2}{r_i}+\frac{1}{4\pi\varepsilon_0}\sum_{i<j}\frac{e^2}{|r_i-r_j|}+\sum_i \xi(r_i)\vec{L}_i\cdot\vec{S}_i \quad (4)$$

where ξ is the spin-orbit coupling coefficient. The ESR in the single crystal system can be characterized by the Hamiltonian H_{ESR}

$$H_{ESR}=H_F+V_{ss}+V_{en}+V_{cf}+V_z \quad (5)$$

where V_{ss}, V_{en}, V_{cf} and V_z are the spin-spin interaction (10^0 cm^{-1}), the magnetic moment of nuclear (10^{-2} cm^{-1}), the crystal fields effect (10^4 cm^{-1}) and the Zeeman effect (10^0 cm^{-1}), respectively. Starting from the electronic configuration of free Cr atoms, Cr^{3+} usually denotes the Cr oxidation state with the half-filled $3d^3$ shell. Within LN crystal structures, this formally threefold ionic charge is distributed over the neighboring host valances and screened by the valence band electrons, so that the ionization threshold is effectively reduced as compared to free Cr ions. Generally, it is incorrect to employ crystal field theory to describe the zero-field-splitting (ZFS) of impurity ground states in LN crystal structures because of the presence of continuum electronic states that hybridize with the atomic Cr orbital. However, the phenomenological form of the crystal field spin Hamiltonian is still correct, even if the true origin of the occurring parameters do not agree with real crystal fields. We consider the ESR spectra at temperatures low enough such that the dynamic process is too slow to affect the ESRLS (the so-called static regime). Therefore, in the static regime, the effective Cr^{3+} ground state manifold of spin state can be described by the spin Hamiltonian which contains the ZFS terms. This Hamiltonian can be represented as

$$H_{sp}=\mu_B(B\cdot\overleftrightarrow{g}\cdot S)+S\cdot\overleftrightarrow{D}\cdot S$$
$$=\mu_B g S_Z B+D\left[S_Z^2-\frac{1}{3}S(S+1)\right] \quad (6)$$

The ESRLS function is calculated to be axially symmetric about the c – axis and analyzed in terms of the spin Hamiltonian with the parameters g = 1.972 and D = 0.395 cm^{-1}. The matrix elements of the spin Hamiltonian are given in Appendix (here, the angles θ and φ are the polar and azimuthal angle, respectively, of the direction of the magnetic field in the principal axes system of $\overleftrightarrow{g}$ and $\overleftrightarrow{D}$ tensors).

Let $|+S;Cr^{3+}\rangle$ be an eigenstate of H_F for a system in which the spin is up and $|-S;Cr^{3+}\rangle$ an eigenstate in which the spin is down with the same orbital. Then the Schrödinger equation is

$$H_F|\pm S;Cr^{3+}\rangle=\left(\varepsilon_{\pm S}\pm\frac{1}{2}\hbar\omega_z\right)|\pm S;Cr^{3+}\rangle \quad (7)$$

We introduce the annihilation and creation operators, $a_{\pm S}$ and $a_{\pm S}^+$, for an eigenstate of H_F. In terms of these operators, we can rewrite the commutator as

$$\begin{aligned}\langle[\sigma_-,\sigma_+(t)]\rangle_{EA}=\langle\sum_{\pm S}\langle -S|\sigma_+(t)|+S\rangle[\{\langle +S|\sigma_+(t)|+S\rangle\\ -\langle -S|\sigma_+(t)|-S\rangle\}a_{-S}^+a_{+S}\\ +\langle +S|\sigma_+(t)|-S\rangle(a_{-S}^+a_{-S}-a_{+S}^+a_{+S})]\rangle_{EA}\\ =\sum_{\pm S}\langle -S|\sigma_-|+S\rangle\langle +S|\sigma_+(t)|-S\rangle(f_{-S}-f_{+S})\end{aligned} \quad (8)$$

where the spin matrices on the right hand side denote electron operators in a Heisenberg representation. For evaluating the right hand side of Eq. (3), we take into account only those terms in Eq. (8) that give a zeroth-order response line; other terms contribute only to give a broad background. We thus will obtain the correct ESRLS absorption. From Eq. (3) we obtain

$$\chi_{+-}''(\omega)=\frac{g_e^2\mu_B^2}{4Vh}\lim_{a\to+0}\mathrm{Re}\sum_{\pm S}(f_{-S}-f_{+S})\langle -S|\sigma_-|+S\rangle\int_0^\infty dt\,\exp(-i\omega t-at)\langle -S|\sigma_+(t)|+S\rangle \quad (9)$$

where $f_{\pm S}=\langle a_{\pm S}^+a_\pm\rangle$, the ordinary Fermi-Dirac distribution function. We see that for the calculation of $\chi_{+-}''(\omega)$, it suffices to calculate

$$\chi_{+-}''(\omega)=\frac{g_e^2\mu_B^2}{4V\hbar}\mathrm{Re}\sum_{\pm S}\frac{f_{-S}-f_{+S}}{i(\omega-\omega_0)+\Pi_{+-}^{ESR}(\omega)} \quad (10)$$

$$\Lambda_{+-}^{ESR}(\omega)\equiv\int_0^\infty\exp(-i\omega t)\langle +S|\sigma_+(t)|-S\rangle=\langle +S|R(\omega)|-S\rangle \quad (11)$$

There may be various methods for evaluating such a quantity that yield almost the same result; however it is most effectively by using the POT adopted by Argyres and Sigel, which is a type of equation of motion method. For an external electromagnetic radiation with a frequency ω applied to the LN crystals, the absorption power delivered to the system is given by

$$P^{ESR}(\omega)=\frac{1}{2}|H_0|^2\,\mathrm{Re}\{\chi_{+-}''(\omega)\} \quad (12)$$

The absorption power is described by the Lorenzian form. The ESRLS is important when it comes to understanding microscopic properties of the electronic state. Most of the other theories require a calculation of the absorption power in order to obtain the ESRLW,

because the whole DESS must be integrated over the electron wave vector. However, in POT, the integration over the electron state appears separately in the numerator and denominator of DESS. This POT has advantageous aspects in that we can directly obtain the ESRLW and well explain the dependence of the temperature and the angle. The absorption power caused by the external field can be expressed by a contribution to DESS that is proportional to the imaginary part of the DESS and the square of the amplitude of an external field. The modulus $|H_0|$ can be treated as a driving force of ESR. It determines the external frequency and the amplitude of the oscillating component of magnetization. The square of $|H_0|^2$ rules the absorption power, i.e., the amplitude of the ESR absorption signals.

We introduce a convenient notation $\hat{O}_{+S-S}=\langle +S|\hat{O}|-S\rangle$ for any arbitrary operator $\hat{O}$. We note that the operator $R(\omega)$ obeys the equation $(\omega-L)^{-1}\sigma_+=R(\omega)$. We must evaluate the quantity $R_{+S-S}(\omega)$. Following Argyres and Sigel, we define the projection operators P_{+-} and their abelian inverse as follows:

$$P_{+-}\hat{O}=\frac{\hat{O}_{+S-S}}{(\sigma_+)_{+S-S}}\sigma_+ \tag{13}$$

$$Q_{+-}=1-P_{+-} \tag{14}$$

We note that $P_{+-}\sigma_+=\sigma_+$, $Q_{+-}\sigma_+=0$, $P_{+-}^2=P_{+-}$ and $P_{+-}Q_{+-}=0$, while we split $R(\omega)=P_{+-}R(\omega)+Q_{+-}R(\omega)$ and then operate with P_{+-} and Q_{+-} separately to obtain with the use of relations

$$(\omega-P_{+-}L)P_{+-}R(\omega)-P_{+-}LQ_{+-}R(\omega)=\sigma_+ \tag{15}$$

$$(\omega-Q_{+-}L)Q_{+-}R(\omega)-Q_{+-}LP_{+-}R(\omega)=0 \tag{16}$$

Solving Eq. (15) for $Q_{+-}R(\omega)$ in terms of $P_{+-}R(\omega)$, we obtain

$$Q_{+-}R(\omega)=G^Q(\omega)Q_{+-}LP_{+-}R(\omega) \tag{17}$$

where $G^Q(\omega)=(\omega-Q_{+-}L)^{-1}=G_F+G_FQ_{+-}L_SG_F+\cdots$, $G_F(\omega)=(\omega-L_F)$.

We substitute Eq. (17) into Eq. (15) and obtain for $P_{+-}R(\omega)$ the equation

$$[\omega-P_{+-}L\{1+G^Q(\omega)Q_{+-}L\}]P_{+-}R(\omega)=\sigma_+ \tag{18}$$

We note that all terms on the left hand side of Eq. (18) are, according to Eq. (13), simple scalar multiples of the operator σ_+. Thus we obtain for the quantity of interest, $R_{+S-S}(\omega)$, the expression

$$\omega-\frac{R_{+S-S}}{(\sigma_+)_{+S-S}}-\frac{\left[L\{1+G^Q(\omega)Q_{+-}L\}\dfrac{R_{+S-S}}{(\sigma_+)_{+S-S}}\sigma_+\right]_{+S-S}}{(\sigma_+)_{+S-S}}=1 \tag{19}$$

Since we are interested in the spin Hamiltonian H_{sp}, it is convenient to introduce the Liouville operators L_F and L_{sp} corresponding to H_F and H_{sp}, respectively, i.e., $L=L_F+L_{sp}$ with $L_F\hat{O}\equiv[H_F,\hat{O}]$ and $L_{sp}\hat{O}\equiv[H_{sp},\hat{O}]$. We then note that $L_F\sigma_+=\omega\sigma_+$, $Q_{+-}L_F\sigma_+=0$, and $(L_FQ_{+-}=\hat{X})_{+S-S}=0$ as it follows from the definitions of L_F and Q_{+-}. We can write Eq. (19) in the form

$$\Lambda_{+-}^{ESR}(\omega)=-iR_{+S-S}(\omega)=\frac{i(\sigma_+)_{+S-S}}{i(\omega-\omega_Z)+\Pi_{+-}^{ESR}(\omega)} \tag{20}$$

Where the ESRLS function $\Pi_{+-}^{ESR}(\omega)$ is defined as follows:

$$\begin{aligned}i\Pi_{+-}^{ESR}(\omega)&=i\Pi_{+-}^{ESR(1st)}(\omega)+i\Pi_{+-}^{ESR(2nd)}(\omega)+i\Pi_{+-}^{ESR(3rd)}(\omega)\\&\quad+i\Pi_{+-}^{ESR(higher)}(\omega)\\&=\frac{1}{(\sigma_+)_{+S-S}}\left[\left\{\sum_n(L_SG^F(\omega)Q_{+-})^nL\right\}\sigma_+\right]_{+S-S}\end{aligned} \tag{21}$$

In order to calculate Eq. (21), the propagator is expanded with a conventional series representation. For the propagator $(\overline{G}^F)_{+-}$, which is contained in Eq. (21) with forbidden transitions $\Delta S\neq\pm1$, we obtain

$$(\overline{G}^F)_{+S-S}=\frac{\hbar}{\varepsilon_\pm+\hbar(\omega-\omega_Z)} \tag{22}$$

$$(\overline{G}^F)_{-S+S}=\frac{\hbar}{\varepsilon_\mp+\hbar(\omega+\omega_Z)} \tag{23}$$

Since we can obtain the ESRLS function directly from the numerical calculations in the POT[Appendix], we can easily analyze ESRLWs for quantum transitions of an external radiation at a frequency of $\nu=9.27$ GHz. We plot the angular and the temperature dependence of LN crystal linewidth for quantum transitions. We studied the angular dependence of linewidths at two different central transitions: $+1/2\leftrightarrow-1/2$ and $+3/2\leftrightarrow-3/2$. The linewidths in the ca and ab planes are shown in Figs. 1 and 2, respectively. We see from Fig. 3 that the linewidths increase monotonically as the temperature increases, and that the linewidths are almost constant in the high-temperature regime. One of the remarkable features of the $+3/2\leftrightarrow-3/2$ transition shown by the ESRLW of LN crystals is that around a certain temperature, which we shall denote by T_{ch}, a

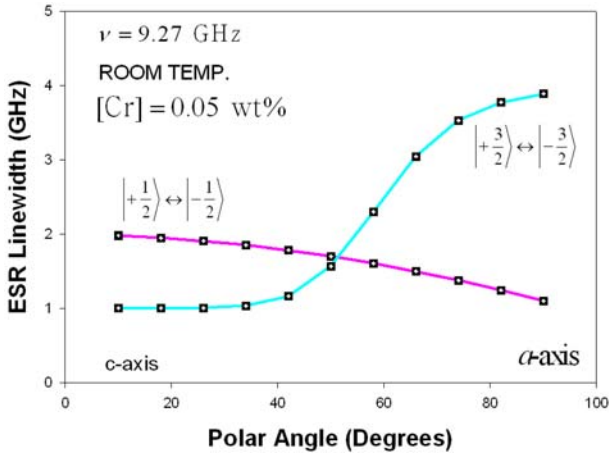

Fig. 1. The polar angle dependence of the linewidths of chromium-doped lithium niobate for transitions +1/2 ↔ –1/2 and +3/2 ↔ –3/2 in ca-plane.

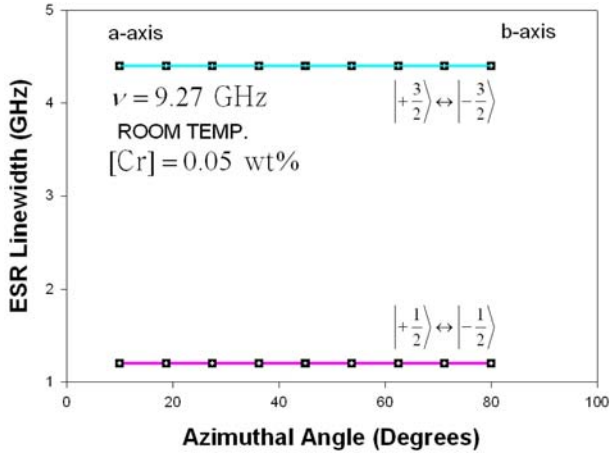

Fig. 2. The azimuthal angle dependence of the linewidths of chromium-doped lithium niobate for transitions +1/2 ↔ –1/2 and +3/2 ↔ –3/2 in ab-plane.

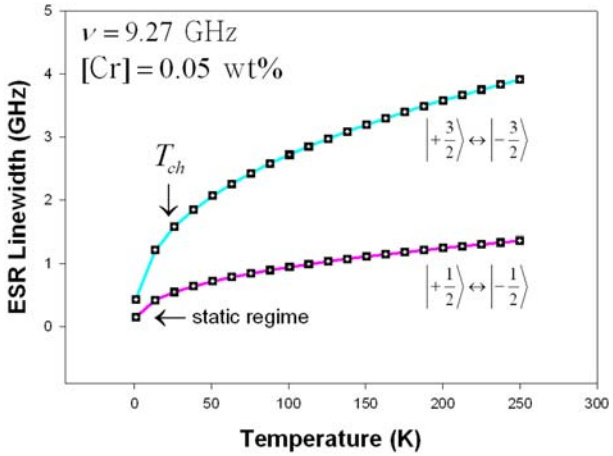

Fig. 3. The temperature dependence of the linewidths of chromium-doped lithium niobate for transitions +1/2 ↔ –1/2 and +3/2 ↔ –3/2 at a frequency of $\nu = 9.27$ GHz.

change in the behavior of the linewidth occurs. It is clear from this feature that there are two regimes in the temperature dependence of the ESRLW: (i) a high-temperature regime in which a slow increase in the linewidth is observed with increasing temperature and (ii) a low-temperature regime in which a sudden increase in the linewidth is observed. The temperature, T_{ch} at which this change occurs seems to be approximately 30 K. Thus, we attribute this feature to the electric dipole interactions of Cr^{3+} ions.

3. Summary

In summary, using numerical calculations, we calculated the ESRLS function for n=1 and 2. The ESRLS of a Cr^{3+} ferroelectric LN material was studied as a function of the temperature and the angle at a frequency of $\nu = 9.27$ GHz (X-band) in the presence of external microwave radiation. The temperature and the angular dependence of the ESRLWs are obtained with the POT developed by Argyres and Sigel. It is easier to obtain the linewidth using this method than using other techniques because it can be obtained directly using the POT, and the approximation $L \rightarrow L_d$ is not needed. In the ca plane, the linewidths show a strong angular dependence, whereas in the ab plane, they are independent of the angle. This result implies that the resonance center has an axial symmetry along the c – axis, and that Cr^{3+} ions are at the sites of axial symmetry, the site of the Li atom, or the site of the Nb atom. From the temperature dependence of the linewidths shown, it can be seen that the linewidths increase as the temperatures increase with external radiation. This result implies that the scattering effect increases with increasing temperature. Thus, the present method can be considered to be more convenient to explain the scattering mechanism as in the case of other optical resonant systems.

Acknowledgment

This research was supported by Basic Science Research Program through the National Research Foundation of Korea(NRF) funded by the Ministry of Education, Science and Technology(NRF-2010-0028207).

Appendix

For $\theta = 0°$, the energy eigenvalues are readily obtained as

$$\varepsilon_{\pm 3/2} = \pm\frac{3}{2} g\mu_B B + D$$

$$\varepsilon_{\pm 1/2} = \pm\frac{1}{2} g\mu_B B - D \qquad \text{(A1)}$$

for $\theta = 90^{o}$ and $\varphi = 0^{o}$, the eigenvalues are also analytically calcuable

$$\varepsilon_{\pm 3/2} = \pm\frac{1}{2} g\mu_B B + \sqrt{g^2\mu_B^2 B^2 \mp g\mu_B D + D^2}$$

$$\varepsilon_{\pm 1/2} = \pm\frac{1}{2} g\mu_B B - \sqrt{g^2\mu_B^2 B^2 \mp g\mu_B D + D^2} \quad \text{(A2)}$$

resonance conditions of ESR transitions are, consequently, as below at $\theta = 0^{o}$,

$$|\frac{3}{2}\rangle \leftrightarrow |-\frac{3}{2}\rangle \ ; \ h\nu = 3g\mu_B B, \ |\frac{1}{2}\rangle \leftrightarrow |-\frac{1}{2}\rangle \ ; \ h\nu = g\mu_B B$$
$$|\frac{1}{2}\rangle \leftrightarrow |-\frac{3}{2}\rangle \ ; \ h\nu = 2g\mu_B B + 2D,$$
$$|-\frac{3}{2}\rangle \leftrightarrow |-\frac{1}{2}\rangle \ ; \ h\nu = -g\mu_B B + 2D \quad \text{(A3)}$$

and at $\theta = 90$ and $\varphi = 0^{o}$,

$$|\frac{3}{2}\rangle \leftrightarrow |-\frac{3}{2}\rangle \ ; \ h\nu = g\mu_B B + \sqrt{g^2\mu_B^2 B^2 - g\mu_B D + D^2} - \sqrt{g^2\mu_B^2 B^2 + g\mu_B D + D^2}$$
$$|\frac{1}{2}\rangle \leftrightarrow |-\frac{1}{2}\rangle \ ; \ h\nu = g\mu_B B - \sqrt{g^2\mu_B^2 B^2 - g\mu_B D + D^2} + \sqrt{g^2\mu_B^2 B^2 + g\mu_B D + D^2} \quad \text{(A4)}$$

The lowest order approximation for n=1 and 2 is given as follows

$$i\Pi_{+-}^{ESR(1st)}(\omega) = \frac{1}{\hbar^2}\sum_{\mu\neq +S}\sum_{\Delta S\neq\pm 1}(\overline{G}^F)_{\mu-S}\langle +S|H_{sp}|\mu\rangle\langle\mu|H_{sp}|+S\rangle + \frac{1}{\hbar^2}\sum_{\mu\neq -S}\sum_{\Delta S\neq\pm 1}(\overline{G}^F)_{+S\mu}\langle -S|H_{sp}|\mu\rangle\langle\mu|H_{sp}|-S\rangle + \frac{1}{\hbar^2}\sum_{\Delta S\neq\pm 1}(\overline{G}^F)_{+S-S}|\langle +S|H_{sp}|+S\rangle|^2 + \frac{1}{\hbar^2}\sum_{\Delta S\neq\pm 1}(\overline{G}^F)_{-S+S}|\langle +S|H_{sp}|+S\rangle|^2 \quad \text{(A5)}$$

$$i\Pi_{+-}^{ESR(2nd)}(\omega) = \frac{1}{\hbar^3}\sum_{\mu\neq +S}\sum_{\Delta S\neq\pm 1}\Big[\sum_{\lambda\neq +S}(\overline{G}^F)_{\mu-S}(\overline{G}^F)_{\mu-S}\langle +S|H_{sp}|\mu\rangle\langle\mu|H_{sp}|\lambda\rangle\langle\lambda|H_{sp}|+S\rangle - (\overline{G}^F)_{\mu-S}(\overline{G}^F)_{+S-S}\langle +S|H_{sp}|\mu\rangle\langle\mu|H_{sp}|+S\rangle\langle -S|H_{sp}|-S\rangle + (\overline{G}^F)_{\mu-S}(\overline{G}^F)_{\mu-S}\langle +S|H_{sp}|\mu\rangle\langle\mu|H_{sp}|+S\rangle\langle +S|H_{sp}|+S\rangle + \frac{1}{\hbar^3}\sum_{\mu\neq +S}\sum_{\Delta S\neq\pm 1}[(\overline{G}^F)_{+S\mu}(\overline{G}^F)_{+S\mu}\langle +S|H_{sp}|+S\rangle\langle -S|H_{sp}|\mu\rangle\langle\mu|H_{sp}|-S\rangle - \sum_{\lambda\neq -S}(\overline{G}^F)_{+S\mu}(\overline{G}^F)_{+S\lambda}\langle -S|H_{sp}|\lambda\rangle\langle\lambda|H_{sp}|\mu\rangle\langle\mu|H_{sp}|-S\rangle] + \frac{1}{\hbar^3}\sum_{\mu\neq +S}\sum_{\Delta S\neq\pm 1}(\overline{G}^F)_{+S-S}(\overline{G}^F)_{+S\mu}\langle +S|H_{sp}|+S\rangle\langle -S|H_{sp}|\mu\rangle\langle\mu|H_{sp}|-S\rangle - \frac{1}{\hbar^3}\sum_{\mu\neq +S}\sum_{\Delta S\neq\pm 1}(\overline{G}^F)_{+S-S}(\overline{G}^F)_{\mu-S}\langle +S|H_{sp}|\mu\rangle\langle\mu|H_{sp}|+S\rangle\langle -S|H_{sp}|-S\rangle \quad \text{(A6)}$$

References

[1] G. Burns, D. F. O'Kane, and R. S. Title, Phys. Rev. **167**, 314 (1968).
[2] N. F. Evlanova, L. S. Kornienko, L. N. Rashkovich, and A. O. Rybaltovskii, Sov. Phys. JEPT. **26**, 1090 (1968).
[3] D. G. Rexford, Y. M. Kim, and H. S. Story, J. Chem. Phys. **52**, 860 (1970).
[4] D. B. Fraser and A. W. Warner, J. Appl. Phys. **37**, 3853 (1966).
[5] H. C. Huang, J. D. Knox, Z. Turski, R. Wargo and J. J. Hanak, Appl. Phys. Lett. **24**, 109 (1974).
[6] F. R. Gfeller, Appl. Phys. Lett. **29**, 655 (1976).
[7] I. P. Kaminow, J. R. Carruthers, E. H. Turner and L. W. Stulz, Appl. Phys. Lett. **22**, 540 (1973).
[8] R. T. smith and F. S. Welsh, J. Appl. Phys. **42**, 2219 (1971).
[9] H. R. Lee, Condens. Matter Phys. **98**, 11008 (1988).
[10] H. Mori, Progr. Theor. Phys. **34**, 399 (1965).
[11] A. Kawabata, J. Phys. Soc. Jpn. **29**, 902 (1970).
[12] A. Lodder and S. Fujita, J. Phys. Soc. Jpn. **25**, 774 (1968).
[13] A. Suzuki and D. Dunn, Phys. Rev. B **25**, 7754 (1982).
[14] J. I. Park and H. R. Lee, J. Korean Phys. Soc. **51**, 623 (2007).
[15] J. I. Park and H. R. Lee, J. Korean Phys. Soc. **53**, 776 (2008).
[16] P. N. Argyres and J. L. Sigel, Phys. Rev. Lett. **31**, 1397 (1973).
[17] R. W. Zwanzig, in Lectures in Theoretical Physics, edited by W. E. Downs and J. Downs, Interscience, New York (1996).
[18] V. M. Kenkre, Phys. Rev. Lett. **29**, 9 (1971).
[19] V. M. Kenkre, Phys. Rev. A **4**, 2327 (1971).
[20] J. Y. Sug, Phys. Rev. B **64**, 235210 (2001).
[21] J. Y. Sug, Phys. Rev. E **55**, 314 (1997).
[22] W. Xiaoguang, F. M. Peeters and J. T. Devreese, Phys. Rev. B **34**, 8800 (1986); X. Wu, F. M. Peeters and J. T. Devreese, ibid. **40**, 4090 (1989); X. J. Kong, C. W. Wei, and S. W. Gu, ibid. **39**, 3230 (1989).
[23] L. P. Gor'kov and G. M. Eliashberg, Sov. Phys. JEPT **21**, 940 (1965).
[24] R. J. Elliott, Phys. Rev. **96**, 266 (1966).
[25] T. W. Kim and J. K. Oh, J. Magnetics **13**, 11 (2008).
[26] T. W. Kim and J. K. Oh, J. Magnetics **13**, 43 (2008).